

# Contrasting prediction skill and predictability of precipitation between Meiyu and rainy season in North China in ECMWF

**Qiong Wu**

Jiangxi Provincial Climate Center

**Zhihai Zheng** (✉ [zhengzh@cma.gov.cn](mailto:zhengzh@cma.gov.cn))

Laboratory for Climate Studies, and National Climate Center, China Meteorological Administration

**Lei Li**

Jiangxi Provincial Meteorological Society

**Shanshan Wu**

Jiangxi Provincial Climate Center

**Yanan Liu**

Jiangxi Provincial Meteorological Sciences Institute

---

## Research Article

**Keywords:** Climate prediction, Prediction skill and predictability, Meiyu and rainy season in North China, ENSO, General circulation in Northern Hemisphere

**Posted Date:** November 29th, 2022

**DOI:** <https://doi.org/10.21203/rs.3.rs-2287264/v1>

**License:**  This work is licensed under a Creative Commons Attribution 4.0 International License.

[Read Full License](#)

**Additional Declarations:** No competing interests reported.

---

**Version of Record:** A version of this preprint was published at Climate Dynamics on June 28th, 2023. See the published version at <https://doi.org/10.1007/s00382-023-06863-y>.

# Abstract

The rainy season in the Yangtze River valley (called Meiyu ) and North China are the main stages with the northward advance of the East Asian summer monsoon. This study investigates the precipitation prediction skills between Meiyu and rainy season in North China using the S2S hindcast data from the European Centre for Medium-Range Weather Forecast (ECMWF) during 2001–2019. The precipitation forecast skill in the Meiyu rainy season is higher than in the rainy season in North China. Moreover, the forecast skill in south of the Yangtze River is better during the Meiyu rainy season, while most areas show negative performance in the rainy season in North China. In the Meiyu rainy season, the single-blocking covering from east of the Lake Baikal to the Sea of Okhotsk in the Asian high latitude and the altitude anomaly over the low latitude ocean area have a significant influence on the precipitation, however, the model's response to these two key areas is different. For the rainy season in North China, the 500 hPa height anomaly over northeast China has a significant impact on the precipitation in the observation, but this influence relationship disappeared in the model. The model biases are both in the circulation and its influence on precipitation. The precipitation forecast skill and their biases in the two rainy seasons are different. Specifically, during the Meiyu rainy season, the prediction skills of circulation in low latitudes are high, and the relationship between circulation and precipitation is also well captured. However, the prediction of circulation in high latitude circulation have less skillful. During the rainy season in North China, the prediction skills of the circulation in the key areas are relatively high, but the relationship between circulation in key areas and precipitation are not captured, or even the opposite. At the same time, it is noted that there are biases in the response of some circulations to the El Nino state in the previous spring at high latitudes in the model. To sum up, the decline in prediction skills with the northward advance of the East Asian summer monsoon indicated that the predictability in high latitudes play a key role.

## 1 Introduction

The monsoonal rainy season in eastern China has distinct regional and temporal characteristics (Ding, 1994; Ding and Chan, 2005; Wang and Ding, 2008). Every year, with the northward advance and southward retreat of the East Asian summer monsoon, southern China, the Yangtze River Basin, and northern China successively enter a period of concentrated precipitation (Wang and Ding, 2008). With the first northward jump of the Western Pacific subtropical high, the East Asian summer monsoon pushes the rain belt toward the Yangtze and Huai River basins in June and July to form plum rains (also called Meiyu) (Qian et al., 2009). Extreme precipitation events such as floods and droughts during the Meiyu rainy season have severely affected the economic development and the people's safety in eastern China. In recent years, the precipitation amount during the Meiyu rainy season has shown an increasing trend in some areas (Wu and Zhan, 2020; Wu et al., 2021). In 2020, the Yangtze and Huai River basins recorded the largest amount of the Meiyu rainy season precipitation since 1961. The direct economic losses and deaths far exceeded other meteorological disasters (Zhang et al., 2020; Chen et al., 2020). With the second northward jump of the subtropical high, the 2nd and 3rd rainy seasons in North China begin in July. The

average duration of the rainy season can reach 32 days and generally accounts for half of the total summer precipitation in the region (Zhao et al., 2017; Chen et al., 2019). The sub-seasonal precipitation variation in the rainy season in North China is often accompanied by an extensive period of rainstorms and floods or drought disasters, which cause great economic loss and casualties. Thus, an accurate precipitation forecast in Meiyu and rainy season in North China is vital for disaster prevention and mitigation.

The direct cause of precipitation anomaly during the Meiyu rainy season is the anomalous atmospheric circulation of the East Asian summer monsoon. The East Asian summer monsoon is mainly affected by the South China Sea monsoon trough, the Meiyu front, the Western Pacific subtropical high, the Qinghai-Tibet high and the northern cold air (Tao and Chen, 1987). The influence of the northern cold air can be explained as the static Rossby wave of the high-altitude subtropical jet, which has a greater impact on the climate of the Meiyu rainy season (Tao and Wei, 2006). When the Okhotsk Sea high forms and stabilizes, the anomalous waves in the middle and high latitudes of Asia and East Asia often cause precipitation anomalies in East Asia during the Meiyu rainy season (Zhang and Tao, 1998). In addition, external forcing such as the ENSO cycle, thermal conditions in the Western Pacific, snow cover and polar ice are closely related to the interannual variation of the plum rains (Tao et al., 1988; Huang and Sun, 1994; Liu and Cao, 1994; Zhang and Tao, 1998; Wu and Qian, 2000; Wei and Song, 2005; Feng et al., 2016). The precipitation in the rainy season in North China has a good relationship with the intensity of the East Asian summer monsoon (Zhu, 1934; Yang et al., 2012; Hao et al., 2016). The circulation anomaly in middle and high latitudes, the position of high-altitude jets, the east-west position of the South Asian high, and the Arctic Oscillation also have an impact on precipitation in the rainy season in North China (Wei et al., 2003; Huang et al., 2006; Wang and He, 2015; Xu et al., 2015; Lu, 2002; Du et al., 2009; Gong et al., 2002), while external forcing such as ENSO, different modes of the Indian Ocean, and land surface conditions of the Qinghai-Tibet Plateau are all related to the anomalous precipitation in the rainy season in North China (Lin and Yu, 1993; Yang and Ding, 2007; Zhang and Tao, 2001; Yu and Chen, 2012).

The development of dynamical model prediction systems contributed to important advances in sub-seasonal to seasonal climate prediction (Saha et al., 2006, 2014; Vitart et al., 2017; Ren et al., 2021). Some models have shown reasonable skill in predicting interannual variability of the Asian monsoon intensity (Jiang et al., 2013; Zhu and Shukla, 2013; Liu et al., 2014, 2015). However, reproducing regional precipitation over China remains a great challenge for climate models (Liu et al., 2013, 2019; Gong et al., 2017; Liang et al., 2019). The low prediction skill is partly associated with the fact that the regional climate processes cannot be well simulated or predicted in climate models. The sub-seasonal prediction skill of the summer precipitation over eastern China is low on average in the Beijing Climate Center (BCC) Atmospheric General Circulation Model (BCC\_AGCM2.2), which is linked to the ability of the model in simulating the western Pacific subtropical high (WPSH). Moreover, as a major contributor to predictability, the spatial pattern and sub-seasonal evolution of the Pacific-Japan region are not well predicted (Liu et al., 2020). In addition, some physical mechanisms in the model show discrepancies, and the impact of some key circulation systems on precipitation has noticeable deviations. In most comprehensive average

forecasts, even for short-term forecasts, the relationship between some dynamic monsoon indices and precipitation patterns is overestimated in the BCC Climate System Model (BCC CSM1.1) (Liu et al., 2015).

The circulation systems that affect Meiyu and rainy season in North China are more complex. The two rainy seasons are affected by low- and mid- and high-latitude circulation systems (Chen et al., 2019). The model's circulation forecasting skills at various latitudes are different. In other words, the circulation in low-latitudes is more predictable than in mid- and high-latitudes (Wu et al., 2017; Ren et al., 2017). The two rainy seasons belong to different stages of the East Asian summer monsoon on China. Circulation system configurations at low- and high- latitudes are different (Chen et al., 2019). The predictability of the two rainy seasons is likely to be different. Therefore, discussing the prediction of key circulation systems in the two rainy seasons and presenting their relationship with precipitation based on models is of great significance for understanding the climatic factors and physical processes that affect the precipitation during the extended periods of the two rainy seasons.

In this study, the difference in the precipitation prediction skills between Meiyu and rainy season in North China are analyzed and compared. The ability of the model (The S2S dataset produced by ECMWF) to predict the key circulation systems that affect precipitation in the rainy seasons and its relationship with precipitation is assessed. The possible reasons for the difference in the prediction skills of precipitation are discussed. Section 2 describes the data and methods. Section 3 presents the contrasting precipitation prediction between Meiyu and rainy season in North China. Section 4 assesses the ability of the model to simulate ENSO and the general circulation associated with precipitation in Meiyu and rainy season in North China. The sources of prediction biases between Meiyu and rainy season in North China are discussed in Section 5. Summary and discussion are given in Section 6.

## 2 Data And Methods

### 2.1 Datasets

The S2S dataset produced by ECMWF is generated on the fly twice a week (Thursday and Monday). The daily extended-range reforecast gives a general view of the forecast for the coming 46 days. Therefore, the rain season data is prepared by summing up the daily values. The reforecast data for 2001–2019 (19 years) is used in this study to evaluate the skill of the precipitation forecast. There are two categories of reforecast configurations used by various centres: the fixed and the on-the-fly. For the fixed, a set of historical reforecasts is produced once by each model version which is then used to calibrate the real-time forecasts. The new reforecast set is produced when the latest forecast model version is released. For the forecasts on the fly, operation centres like ECMWF update the version of the model several times a year for consistency between real-time and reforecasts. The reforecast are used to calibrate and continuously produce real-time forecasts. More details are available at <https://confluence.ecmwf.int/display/S2S/ECMWF+Model>. In the current work, we utilized the S2S reforecast version CY46R1, which based on 51 members, runs twice a week (Monday and Thursday at 00Z) up to day 46.

The observation used for model evaluation is the ERA-Interim daily precipitation and atmospheric variables reanalysis data (ERA-Interim, Dee et al., 2011). Cumulative precipitation reanalysis is produced in meter (m) at 12-hourly temporal samplings and is converted to millimeters (mm).

## 2.2 Duration and area of the two rainy seasons

Meiyu and rainy season in North China are the main rainy season processes in China's flood season, and a large number of studies have been carried out on the two typical rainy seasons. Referring to previous studies (Chen et al., 2019; Hu et al., 2010; Ma et al., 2011; Yu et al., 2019), the rainy season of Meiyu is selected between 110 ° E – 125 ° E and 25 ° N – 35 ° N, and the rainy season in North China is selected between 110 ° E – 125 ° E and 35 ° N – 43 ° N. Moreover, for taking into account the comparative analysis of the rainy seasons, the same rainy season duration (5 weeks) is selected to study the difference in the precipitation prediction skills between Meiyu (June 8 to July 12) and rainy season in North China (July 13 to August 16).

### 2.3 Methods

The percentage anomaly between the observed and predicted variables is defined as the departure from the two rainy seasons' multi-year mean climatology (2001 to 2019), calculated as follows:

$$DIFF(\%) = \frac{F-X}{X} \times 100 \quad (1)$$

where,  $F$  is the ensemble forecast value and  $X$  is the observation value.

The forecasting skills are assessed by the anomaly correlation coefficient (ACC), the temporal correlation coefficient (TCC) and the root-mean-square error (RMSE). The definition of blocking high-pressure is determined according to the regulations of the NCC for real-time monitoring of blocking high-pressure in the Northern Hemisphere, which is a method of height field gradient difference improved by Tibaldi and Molteni (Zhao 2000). A certain longitude index can be calculated as follows:

$$GHG = \frac{z(\varphi_1) - z(\varphi_2)}{\varphi_1 - \varphi_2} \quad (2)$$

where  $Z$  is the geopotential height,  $\varphi_1$  and  $\varphi_2$  are latitudes,  $\varphi_1 = 60 + \delta$ ,  $\varphi_2 = 40 + \delta$ , where  $\delta$  can be  $-5$ ,  $0$ , and  $5$ . The blocking high-pressure of a certain key area is the average blocking high-pressure within the longitude interval of the key area.

## 3 Contrasting Prediction Of Precipitation Between Meiyu And Rainy Season In North China

To compare the precipitation prediction between Meiyu and rainy season in North China, Fig. 1 shows the distributions of the ACC between ERA data and S2S predictions for different lead times and ensemble-averaged forecasts. By comparing different lead time (0 4 7 and 11 days ahead) forecasts, it is found that the Meiyu rainy season have better precipitation forecasting skills than the rainy season in North China (Fig. 1a). During the Meiyu rainy season, the forecast effect is the best for 0 day lead time, and the multi-year average ACC exceeds 0.2. The highest ACC in the rainy season in North China is 0.05 (4 days ahead), and the lowest value is -0.16 (11 days ahead). From the ensemble forecasts of 204 members with 4 lead times, obvious interannual differences are observed in the precipitation forecasting skill of the

two rainy seasons (Fig. 1b). During the Meiyu rainy season, ACC reaches up to 0.61 in the year with a good forecast effect (2015). On the other hand, only  $-0.27$  is noted in the year with a poor effect (2006). In the rainy season in North China, the highest ACC is up to 0.47 (2014), while the lowest value is only  $-0.48$  (2012). The precipitation forecasting skill during the Meiyu rainy season for 2001–2019 is generally better than in the rainy season in North China. From the multi-year average, the ACC of the ensemble forecast is 0.23 during the Meiyu rainy season and  $-0.06$  during the rainy season in North China. That is, there are obvious differences between the two rainy seasons in terms of the ensemble forecasting skill of precipitation.

In the following analysis, the rainy season predictions of 204 members with leads of 0, 4, 7 and 11 days initialized with slightly different atmospheric initial conditions are used.

Figure 2a, d respectively show the percentage of deviation between the model and observed precipitation in the two rainy seasons. It can be seen that there is a deviation in the model prediction of precipitation in the two rainy seasons. During the Meiyu rainy season, most of the northern areas have more precipitation. Precipitation is 30–60% more to the north of Anhui and is generally less to the south of the Yangtze River, and 15–30% less in northern Fujian, most of Zhejiang and the adjacent sea areas. In the rainy season in North China, precipitation is 10–40% more in most areas and 10–30% less in Shanxi and eastern Shandong. From the RMSE of total precipitation in the two rainy seasons (Fig. 2b, e), RMSE is up to 120–150 in areas with large precipitation deviations. RMSE is relatively small in the rainy season in North China (only 100–130 in the center). From the TCC between the observed and model-predicted precipitation in the two rainy seasons (Fig. 2c, f), there are obvious differences in the model forecast effect of during the precipitation Meiyu rainy season between the north and south. That is, the forecast effect in areas to the south of the Yangtze River is better, with a TCC of 0.1–0.6, and most areas passed the 95% confidence level test. The forecast effect in the areas north of the Yangtze River is poor, with TCC  $< 0$  in most areas. The model does not have high forecasting skills for the precipitation in the rainy season in North China. Most areas show a negative correlation, and almost all areas do not pass the significance level test. The TCC negative value center is located north of Hebei, with TCC between  $-0.65$  and  $-0.5$ .

## **4 Prediction Of General Circulation Associated With Precipitation During Meiyu And Rainy Season In North China**

### **4.1 The Meiyu rainy season**

Figure 3a shows the climatological large-scale circulation during Meiyu rainy season. During this season, the western Pacific subtropical high is distributed zonally, with its ridgeline extending from southern Japan to southern China. The high latitude circulation over Asia exhibits a single-blocking characteristic. That is, a blocking high covering the region from east of the Lake Baikal to the Sea of Okhotsk. A low trough extends from the south of the blocking high to the middle latitudes, which is advantageous for bringing cold air to the north of the Meiyu area and its interactions with the East Asian summer monsoon

(Ding et al., 2020). Figure 3c shows the model-predicted climatological large-scale circulation during the Meiyu rainy season. When the subtropical high forms, the single blocking high pressure in high latitudes and the distribution of low troughs in the south are well simulated. To further identify the key areas of circulation at 500 hPa that affect precipitation during the Meiyu rainy season, the observed (model-predicted) precipitation index is used to regress the observed (model-predicted) 500 hPa height. From the regressed observation field (Fig. 3b), it can be seen that high latitude areas such as the Lake Baikal and low-latitude areas from the South China Sea to the Western Pacific display positive and significant correlation. The correlation is negative in middle latitudes but does not pass the significance level test, which shows the beneficial influence of the active trough on precipitation. The distribution in the regressed model field is similar (Fig. 3d). The correlation is positive, negative and positive from high to low latitudes. However, the center of positive correlation in high latitudes is obviously easterly. The negative correlation in middle latitudes is stronger and significant. The regressed height field in low latitudes is basically consistent with the observation.

Based on the above analysis, the effect of two key circulation configurations (high-latitude blocking high pressure (BHP) at 500 hPa and height anomaly field over low latitude ocean areas) on precipitation during the Meiyu rainy season are discussed. According to the observation and model performance,  $\delta$  is  $-5$  in the specific calculation formula of BHP. The average BHP in the longitude range from the east of Lake Baikal to the Okhotsk Sea ( $110^{\circ}$  E - $140^{\circ}$  E, the area between the lines in Fig. 4a) is selected to represent the BHP in this key area. Figure 4a shows the 500 hPa height anomaly field regressed by BHP in the observation. The central distribution shows a single blocking high pressure. The model regression portrays the key area configuration, and the “+” distribution in the middle and high latitudes is significant. In the regressed observed precipitation field by BHP, there is a significant positive correlation in the south and a negative correlation in the north. That is, the north-south inverse characteristic is very obvious (Fig. 4b). In the regressed model precipitation field by BHP, precipitation is small in size and is scattered in the southern area. The negatively correlated area in the north is significantly more northerly and almost no areas passed the significance level test (Fig. 4d).

During the Meiyu rainy season in East Asia, the western Pacific subtropical high is distributed zonally (Ding et al., 2020), and the ridgeline along  $120^{\circ}$ E jumps to  $22^{\circ}$ N and the areas north (Xu et al., 2001). To discuss the effect of low latitudes 500 hPa height anomaly on precipitation during the Meiyu rainy season, the significant positive correlation area is selected from the most obvious subtropical high area ( $120^{\circ}$ E - $165^{\circ}$ E,  $15^{\circ}$ N - $25^{\circ}$ N) in Fig. 3b, d. The subtropical high (SH) is the average height anomaly within the area (black box in Fig. 5a). Figure 5a and c show the regressed 500 hPa height distribution by SH in the observation and model, respectively. The indices all well display the distribution of anomalous key areas in low latitudes. In the observed precipitation field regressed by SH (Fig. 5b), there is a significant positive correlation in the central and southern areas and a negative correlation in the northeastern and northwestern areas. In the regression field of model precipitation by SH (Fig. 5d), the overall distribution of precipitation is similar to the observed regression field. That is, it is distributed zonally between  $26^{\circ}$ N and  $30^{\circ}$ N, and the central large area is significant.

## 4.2 Prediction in Rainy season in North China

Previous studies have shown that the zonal “+ – +” wave train structure in the Ural Mountains of Eurasia, the area between Lake Balkhash and Lake Baikal, and the area from the Bohai Bay to the Japanese archipelago is conducive to more precipitation in the rainy season in North China. Wei et al. (2003) and Wang and He (2015) called this wave train the EU teleconnection pattern. In order to analyze the key areas of circulation affecting precipitation in the rainy season in North China, the observed (model-predicted) precipitation index is used to regress the observed (model-predicted) 500 hPa height field. From the regressed field (Fig. 6a), it can be seen that the Ural Mountains and Northeast China are significant and positive. In middle latitudes, the correlation is negative but insignificant. In the regressed model field, there is an opposite distribution in high latitudes (Fig. 6d), and the correlation is negative in the Ural Mountains and Northeast China, which indicates that the physical mechanisms of circulation and precipitation in the model are different.

Zhao et al. (2017) believe that the relationship between the normal and anomaly from the Bohai Bay to the Japanese archipelago and the rainy season in North China is the most significant, reflecting the northwesterly and northerly distribution of the subtropical high over the northwestern Pacific, which is conducive to the transport of water vapor from the South China Sea and the tropical Pacific to North China. Combined with the significant area of the response areas in Fig. 6a, the high pressure index HP is constructed as the average of 500 hPa height anomaly in the area (120°E -135°E, 40°N -50°N, black box in Fig. 6b) and is standardized to regress the 500 hPa height anomaly field in the same period (Fig. 6b). The central distribution shows that the normal and anomalous distribution in the Ural Mountains and Northeast China is consistent with the distribution of key areas in the height field regressed by precipitation. The regression field of the model shows the normal and anomalous distribution of the two areas, both passing the significance test.

In the observed precipitation field regressed by HP, there is positive correlations in the whole area, and most of the northern central area are significant. In the regression field of the model precipitation, the positive correlation area is very small, with a small magnitude. There is a negative and significant correlation in the east. It is seen that there is a big difference between the observation and model in the relationship between HP and precipitation in the rainy season in North China.

## 4.3 Sources of prediction biases between Meiyu and rainy season in North China

Figure 7a shows the distribution of the 500 hPa height average field deviation between the model and observation during the Meiyu rainy season from 2001 to 2019. There is an obvious positive anomaly in middle latitudes and a negative anomaly in the high and low latitudes. The regional deviation is obvious in the middle and high latitude key areas, and is smaller in the low latitude western Pacific. From the observed and model 500 hPa height TCC field, it can be seen that the correlation in low latitudes is higher than in high latitudes, and the TCC in the low latitude key areas reaches 0.60–0.89, all passing the



significance test. There are differences in the simulation effect of circulation between middle and high latitudes with the BHP index (Fig. 7b). The correlation is significant within a certain longitude range in middle latitudes, and TCC is 0.22–0.78. The correlation is low and insignificant from the east of Lake Baikal to the Okhotsk Sea, and TCC is only 0.06–0.29.

The distribution of the 500 hPa height average field deviation between the model and observation in the rainy season in North China from 2001 to 2019 is shown in Fig. 7c. The middle and high latitudes deviation distribution is similar to that of the Meiyu rainy season. That is, there is a negative anomaly in high latitudes and a zonal positive anomaly in middle latitudes. From the observed and model-predicted 500 hPa height TCC field in the rainy season in North China (Fig. 7d), it can be seen that the simulation effect over China is better and most areas are significant. In addition, the TCC of the key circulation area over Northeast China is 0.24–0.68.

The circulation deviation of the model will inevitably lead to different simulation effects of the circulation index in each key area. From the simulation effect of each index (Table 1), the simulation effect of SH index in low latitudes is the best, and the correlation coefficient with the observation is 0.86. BHP index is only 0.29, and the high-latitude area constituting the BHP index is marked as BHP.1, while the middle-latitude area is BHP.2. The correlation coefficient of BHP.2 is 0.64, while the simulation effect of BHP.1 is low (0.2). It can be seen that during the Meiyu rainy season, the index in the high latitude key area is low. The simulation effect of the circulation index HP in the key area in the rainy season in North China is better, with a correlation coefficient of 0.48.

Table 1  
Correlations between indices from ERA-Interim and S2S.

Meiyu		Rainy season in North China		
SH	BHP	BHP.1	BHP.2	HP
0.86	0.29	0.2	0.64	0.48

The correlation coefficient of the regional precipitation index during the Meiyu rainy season is 0.43, while that of the rainy season in North China is only 0.01. The relationship between the circulation index and precipitation in each key area in the two rainy seasons in the observation and model is further analyzed (Table 2). The correlation coefficient between SH index and precipitation in low latitudes is the highest during the Meiyu rainy season, reaching 0.65 and 0.76 in ERA-Interim and S2S, respectively. The correlation coefficient between the BHP index and precipitation is 0.40 and 0.41, respectively. It can be seen that the relationship between each index and precipitation in the observation and model during the Meiyu rainy season is consistent. For the rainy season in North China, the relationship between precipitation and each index in the circulation key area show an opposite characteristic. In the observation, the correlation coefficient between the HP index and precipitation is 0.49 and significant. In

the model, the correlation coefficient between HP index and precipitation is -0.26. It can be seen that the effect of this key area on the rainy season in North China is not reproduced by the model.

Table 2 Correlations between indices and precipitation from ERA-Interim and S2S.

Correlation	Index	Meiyu		Rainy season in North China
		SH	BHP	HP
index.ERA & P.ERA		0.65	0.4	0.49
index.S2S & P.S2S		0.76	0.41	-0.26

## 5 Prediction Of Enso During Meiyu And Rainy Season In North China

### 5.1 The Meiyu rainy season

The precipitation during the Meiyu rainy season is affected by ENSO (Wei and Song., 2005; Liang et al., 2018; Chen et al., 2019). The observed standardized precipitation index (regional average precipitation) during the Meiyu rainy season from 2001 to 2019 are used to regress the distribution of observed SST anomaly field in the previous winter (December to February), spring (March to May) and summer (June to August). In winter, there is a significant (at 95% confidence level) positive correlation area in the equatorial central and eastern Pacific (Fig. 8a). In spring (Fig. 8b), the positive correlation area in the equatorial eastern Pacific disappears and the range of positive correlation in the equatorial central Pacific becomes smaller. In summer (Fig. 8c), the significant positive correlation areas in the equatorial central and eastern Pacific in winter and spring disappear. The model standardized precipitation index are used to regress the distribution of SST anomaly field in model. In winter, the equatorial central and eastern Pacific has a large positive correlation area (Fig. 8d). In spring, the large positive correlation area in the equatorial eastern Pacific also disappears and the range of positive correlation in the equatorial central Pacific is larger (Fig. 8e). As shown in the regressed SST anomaly field in summer, a negative correlation appears in the equatorial eastern Pacific but is not significant (Fig. 8f). The response of precipitation during the Meiyu rainy season to SST changes in the equatorial central and eastern Pacific Ocean are relatively consistent in observations and models, when the equatorial Central Pacific and East Pacific are warmer in winter, while El Nino is weaker in spring and summer, it is expected that the rainfall will be greater in the rainy season.

The equatorial central and eastern Pacific are key areas significantly correlated with the Meiyu rain season. The Niño3.4 index from the previous winter, spring and summer is used to regress the 500-hPa height anomaly field during the Meiyu rainy season (Fig. 9). In the regression field of the Niño 3.4 index from the previous winter, the correlation distribution between observation and model in low, middle and high latitudes is similar.; The difference is that the positive correlations over the Western Pacific region and the Outer Mongolia region are significant (Fig. 9a),while they are not significant in the model (Fig. 9d). In the regression field of the Niño 3.4 index from the previous spring (Fig. 9b), the most significant positive correlation areas between the observation and model are consistent in low latitudes.

But, there are large differences in the high latitudes. In the model, the significant positive correlation areas disappear west of Baikal Lake. In the regression field of the Niño 3.4 index from the previous summer, the circulation relationship is well simulated.

Refer to Fig. 3b, It can be seen that the SST of the equatorial Middle East Pacific Ocean in the previous winter and spring presented an El Niño state, which could form a circulation structure conducive to precipitation during the Meiyu period. In the model, the circulation responds well to the El Niño state in the previous winter, but has errors in the high latitude for the El Niño state in the previous spring. For summer, the circulation structure affected by SST is not the key system of Meiyu.

In order to further study the relationship between SST anomaly in the equatorial Pacific and precipitation during the Meiyu rainy season, the Niño3.4 index of SST in the previous winter, spring and summer is used to regress the precipitation field during the Meiyu rainy season (Fig. 10). Regression with the Niño3.4 index in the previous winter, the correlation in the northern central area is significant at 95% confidence test in observed (Fig. 10a), while the correlation is significant in the southeast in the model. Regression with the Niño3.4 index in the previous spring (Fig. 10b), the correlation is positive in the south in observed, mostly passing the 95% confidence level test, while there is a negative correlation in the north. In the regressed model precipitation field, the correlation is positive in the south, but the magnitude is relatively small. There is a positive correlation in the north, with few significant areas. As shown precipitation field regressed by the summer Niño3.4 index (Fig. 10c), there is an obvious reversed characteristic in the north and south in observed, but the correlation is insignificant. In the regressed model precipitation field, there is a positive correlation in the whole area and the precipitation magnitude in the south is obviously smaller.

## 5.2 Prediction in Rainy season in North China

It is found that the anomalously more precipitation in the rainy season in North China usually occurs in the year when El Niño ends and turns to La Niña. In comparison, the anomalously less precipitation in the rainy season in North China usually appears in the year when the cold water of the equatorial central and eastern Pacific develops into El Niño (Zhao et al., 2017). Figure 11a-c shows the distribution of the observed SST anomaly field in the previous winter, spring and summer regressed by the observed standardized precipitation indices (regional average precipitation) in the rainy season in North China. In winter, there is a positive but insignificant correlation area in the equatorial central and eastern Pacific (Fig. 11a). In spring (Fig. 11b), the positive correlation area in the equatorial central and eastern Pacific almost disappears and a negative correlation area appears. In summer (Fig. 11c), there is an obvious negative correlation area in the equatorial central and eastern Pacific, and the correlation is significant in some areas of the equatorial eastern Pacific. Consistent with the observation, in the regressed SST anomaly field in the previous winter by the model precipitation index, there is a positive correlation area in the equatorial central and eastern Pacific (Fig. 11d). In spring, the positive correlation area in the equatorial central and eastern Pacific disappears and a negative correlation area appears in the equatorial eastern Pacific (Fig. 11e). In summer, a uniform negative but insignificant correlation area

appears in the equatorial eastern Pacific (Fig. 11f). When El Niño decays in the early winter and La Niña develops in that year, precipitation is higher in the rainy season in North China; otherwise, it is less. This is consistent with the previous research conclusion, but the relationship in the figure is not significant.

## 6 Summary And Discussion

This study assessed the interannual precipitation prediction skills between Meiyu and rainy season in North China Using the ECMWF's ERA-Interim reanalysis data and the S2S hindcast data for 2001–2019. It was found that there is an obvious difference between different years in the forecasting skill of precipitation in the two rainy seasons. In most years, the precipitation forecasting skill is higher during the Meiyu rainy season than during the rainy season in North China. During Meiyu, the forecast effect is better in the area to the south of the Yangtze River, and the TCC is up to 0.4–0.6 in some areas. The forecast skill during the rainy season in North China is low, most areas even show negative skills.

There is a certain difference between the observation and model precipitation magnitude in the rainy season in North China, and the difference in the position of the precipitation center is also obvious. During Meiyu, the responses of the model predicted precipitation to circulation in key areas in various latitudes are different. Moreover, the model-predicted precipitation in response to the blocking high-pressure in middle and high latitudes is scattered. The precipitation in response to the 500 hPa height anomaly in low latitudes is close to the observed precipitation. The 500 hPa height anomaly over Northeast China has a significant impact on precipitation in the rainy season in North China, but this impact is not reproduced by the model.

The model biases are both in the circulation and its influence on precipitation. The precipitation forecast skill and their biases in the two rainy seasons are different. During Meiyu, The prediction skills of circulation in low latitudes are high, and the relationship between circulation and precipitation is also well captured. However, the prediction of circulation in high latitude circulation have less skillful. During the Huabei rainy season, the prediction skills of the circulation in the key areas is relatively good, but the relationship between circulation in key areas and precipitation are not captured, or even the opposite.

The precipitation in the Meiyu rainy season has a good response to the SST changes in the equatorial central Pacific and eastern Pacific in the previous winter and spring in both the observation and model, but some circulation in Meiyu have different responses to the El Nino state in the model, the circulation responds well to the El Nino state in the previous winter, but has errors in the high latitude for the El Nino state in the previous spring. For the rainy season in North China, the response of precipitation to the SST changes in the equatorial central Pacific and eastern Pacific is not significant.

Numerical models inevitably have errors. It is becoming increasingly difficult to improve the models to further increase the forecasting skill. Many studies used statistical methods to improve the forecasting ability of dynamic models (Saha, 1992; Ren, 2006; Zheng et al., 2009; Feng et al., 2013). The main idea is to use past observation or forecast data to establish the statistical relationship between circulation fields and surface element fields, and then to output circulation fields by the model to indirectly predict surface

element fields (Feddersen and Uffe, 2005; Li and Chen, 1999; Wei and Huang, 2010; Guo and Li, 2012). In this paper, the difference in the precipitation predictability between Meiyu and rainy season in North China was discussed. The sources of biases in the two regions are also analyzed, which has important implications for the localized interpretation of models in the future. During Meiyu, more attention should be paid to the circulation deviation in each key area. In the rainy season in North China, it should be noted that, the predictability of high latitude regions on the sub seasonal time scale plays a key role.

It should be noted that there are often differences in precipitation in the two rainy seasons. During Meiyu, the anomalous activity of the East Asian summer monsoon is accompanied by the southward or northward movement of the East Asian monsoon system, resulting in different rain belt positions. This corresponding relationship between circulation and precipitation is often more specific and obvious than the circulation throughout the rainy season. In fact, floods in the Jianghuai region occur in different regions (Qian et al., 2007). In 2020, the precipitation during Meiyu is mainly concentrated in the middle and lower reaches of the Yangtze River (Liu and Ding, 2020). Therefore, it is necessary to explore the ability of models to predict different types of precipitation in the rainy season and their possible differences.

## Declarations

**Funding** This work is supported by the National Natural Science Foundation of China (U2142207, 41875101) and the National Key R&D Program of China (2017YFC1502303).

**Competing Interests** The authors have no relevant financial or non-financial interests to disclose.

**Author Contributions** Material preparation, data collection and analysis were performed by Qiong Wu. The conception of the study was contributed by Zhihai Zheng and the analysis with constructive discussions were performed by Lei Li, Shanshan Wu and Yanan Liu. All authors read and approved the final manuscript.

**Data Availability** The data that support the findings of this study are openly available in ECMWF at [<https://apps.ecmwf.int/datasets/>].

**Acknowledgments** The authors thank ECMWF for providing the S2S data used in this study. We are extremely grateful to the anonymous reviewers for their valuable comments on this paper.

## References

1. Chen L J, Li W J, Zhang P Q, et al (2003) Application of a new downscaling model to monthly precipitation forecast [J]. *Journal of Applied Meteorological Science*. 14(6): 648-655.
2. Chen L J, Zhao J H, Gu W, et al (2019) Advances of research and application on major rainy seasons in China [J]. *Journal of Applied Meteorological Science*. 30(4):385-

- 400.<https://doi.org/10.11898/1001-7313.20190401>.
3. Chen T, Zhang F H, Yu C, et al (2020) Synoptic analysis of extreme Meiyu precipitation over Yangtze river basin during June-July 2020 [J]. *Meteorological Monthly*. 46(11):1415-1426.
  4. Chu K Z (1934) The enigma of Southeast Monsoon in China [J]. *Acta Geographica Sinica*. 1(1):1-27.
  5. Dee D P (2011) The ERA-Interim reanalysis: configuration and performance of the data assimilation system [J]. *Quarterly Journal of the Royal Meteorological Society*. 137:553– 597.
  6. Ding Y H (1994) *Monsoons over China* [M]. London: Kluwer Academic Publishers: 135– 136.  
<https://doi.org/10.1007/BF02666553>
  7. Ding Y H, Chan J C L (2005) The East Asian summer monsoon: an overview [J]. *Meteorology and Atmospheric Physics*. 89(1-4):117– 142. <https://doi.org/10.1007/s00703-005-0125-z>
  8. Ding Y H, Liang P, Liu Y J, et al (2020) Multiscale Variability of Meiyu and Its Prediction: A New Review [J]. *Journal of Geophysical Research: Atmospheres*. 125(7). DOI:10.1029/2019JD031496
  9. Du Y, Zhang Y C, Xie Z Q (2009) Location variation of the east asia subtropical westerly jet and its effect on the summer precipitation anomaly over Eastern China [J]. *Chinese Journal of Atmospheric Sciences*. 33(3):581-592.
  10. Feddersen H, Uffe A (2005) A method for statistical downscaling of seasonal ensemble predictions [J]. *Tellus*. 57A:398-408. <https://doi.org/10.1111/j.1600-0870.2005.00102.x>
  11. Feng G L, Zhao J H, Zhi R, et al (2013) Recent progress on the objective and quantifiable forecast of summer precipitation based on dynamical-statistical method [J]. *Journal of Applied Meteorological Science*. 24(6): 656-665.
  12. Feng J, Li J P, Zheng F, et al (2016) Contrasting Impacts of Developing Phases of Two Types of El Niño on Southern China Rainfall [J]. *Journal of the Meteorological Society of Japan Ser II*. 94(4):359-370. DOI:10.2151/jmsj.2016-019
  13. Gong D Y, Zhu J H, Wang S W (2002) Significant correlation between summer precipitation in the Yangtze River Basin and the Prior Arctic Oscillation [J]. *Chinese Science Bulletin*. 47(7):546-549.
  14. Gong Z Q, Dogar M , Qiao S B, et al (2017) Limitations of BCC\_CSM's ability to predict summer precipitation over East Asia and the Northwestern Pacific [J]. *Atmospheric Research*, 193:184-191. <https://doi.org/10.1016/j.atmosres.2017.04.016>
  15. Guo Y, Li J P (2012) A time-scale decomposition statistical downscaling model: Case study of North China rainfall in rainy season [J]. *Chinese Journal of Atmospheric Sciences*. 36(2): 385-396.
  16. Hao L S, Ding Y H, Min J Z (2016) Relationship between summer monsoon changes in East Asia and abnormal summer rainfall in North China [J]. *Plateau Meteorology*. 35(5):1280-1289.
  17. Huang J P, Ji M X, KazHIGUCHI, et al (2006) Temporal Structures of the North Atlantic Oscillation and Its Impact on the Regional Climate Variability [J]. *Advances in Atmospheric Sciences*, 23(1):23-32.  
[doi:CNKI:SUN:DQJZ.0.2006-01-004](https://doi.org/10.1007/s00036-006-0100-4)
  18. Huang R H, Sun F Y (1994) Impacts of the Thermal State and the Convective Activities in the Tropical Western Warm Pool on the Summer Climate Anomalies in East Asia [J]. *Chinese Journal of*

- Atmospheric Sciences, 18(2):141-151. [doi: 10.3878/j.issn.1006-9895.1994.02.02](https://doi.org/10.3878/j.issn.1006-9895.1994.02.02)
19. Hu Y M, Ding Y H, Liao F (2010) A classification of the precipitation patterns during the Yangtze-Huaihe meiyu period for the recent 52 years [J]. *Acta Meteorologica Sinica*, 68(2):235-247. <https://doi.org/10.11676/qxxb2010.024>
  20. Jiang X, Yang S, Li Y, et al (2013) Seasonal-to-interannual prediction of the Asian summer monsoon in the NCEP climate forecast system version 2 [J]. *Journal of Climate*. 26:3708–3727. <https://doi.org/10.1175/JCLI-D-12-00437.1>
  21. Liang P, Chen L J, Ding Y H, et al (2018) Relationship between long-term variability of Meiyu over the Yangtze River and ocean and Meiyu's predictability study. *Acta Meteorologica Sinica* [J]. 76(3):379-393.
  22. Liang P, Hu Z Z, Liu Y, Yuan X, Li X, Jiang X (2019) Challenges in predicting and simulating summer rainfall in eastern China [J]. *Climate Dynamics*. 52(3-4):2217–2233. <https://doi.org/10.1007/s00382-018-4256-6>
  23. Lin X C, Yu S Q (1993) El nino and rainfall during the flood season (June-August) in China [J]. *Chinese Academy of Meteorological Sciences*, 51(4):434-441.
  24. Liu X W, Wu T, Yang S, et al (2014) Relationships between interannual and intraseasonal variations of the Asian-western Pacific summer monsoon hindcasted by BCC\_CSM1. 1(m) [J]. *Advances in Atmospheric Sciences*. 31:1051–1064. <https://doi.org/10.1007/s00376-014-3192-6>
  25. Liu X W, Wu T, Yang S, et al (2015) Performance of the seasonal forecasting of the Asian summer monsoon by BCC\_CSM1.1(m) [J]. *Advances in Atmospheric Sciences*. 32:1156–1172. <https://doi.org/10.1007/s00376-015-4194-8>
  26. Liu Y, Hong J, Liu C, et al (2013) Meiyu flooding of Huaihe River valley and anomaly of seasonal variation of subtropical anticyclone over the western Pacific [J]. *Chinese Journal of Atmospheric Sciences*. 37:439–450. <https://doi.org/10.3878/j.issn.1006-9895.2012.12313>
  27. Liu Y, Ke Z, Ding Y (2019) Predictability of East Asian summer monsoon in seasonal climate forecast models [J]. *International Journal of Climatology*. 39:5688-5701. <https://doi.org/10.1002/joc.6180>
  28. Liu Y, Hu Z Z, Wu R, et al (2021) Subseasonal prediction and predictability of summer rainfall over eastern China in BCC\_AGCM2.2 [J]. *Climate Dynamics*. 56(7):2057-2069.
  29. Liu Y Y, Ding Y H (2020) Characteristics and possible causes for the extreme Meiyu in 2020 [J]. *Meteorological Monthly*. 46(11):1393-1404.
  30. Liu Z X, Cao H X (1994) Teleconnection between arctic ice and Meiyu over the middle and lower reaches of Changjiang river [J]. *Meteorological Monthly*. 20(11):21-24. <https://doi.org/10.7519/j.issn.1000-0526.1994.11.004>
  31. Li W J, Chen L J (1999) Research on reexplanation and reanalysis method of dynamical extended range forecast products [J]. *Acta Meteorologica Sinica*. 57(3):338-345. [doi: 10.11676/qxxb1999.032](https://doi.org/10.11676/qxxb1999.032)
  32. Lu R Y (2002) Separation of interannual and interdecadal variations of rainfall in North China 2002[J]. *Chinese Journal of Atmospheric Sciences*. 26(5):611-624.

33. Ma Y, Chen W, Wang L (2011) A comparative study of the interannual variation of summer rainfall anomalies between the Huaihe Meiyu season and the Jiangnan Meiyu season and their climate background [J]. *Acta Meteorologica Sinica*,69(2):334-343.
34. Qian W H, Zhu J, Wang Y G, et al (2009) Regional relationship between the Jiang-Huai Meiyu and the equatorial surface-subsurface temperature anomalies [J]. *Chinese Science Bulletin*. 54 (1): 113–119, <https://doi:10.1007/s11434-008-0410-6>
35. Qian Y F, Wang Q Q, Huang D Q (2007) Studies of floods and droughts in the Yangtze-Huaihe River Basin [J]. *Chinese Journal of Atmospheric Sciences*. 31(6): 1279-1289.
36. Ren H L, Wu J, Zhang S, et al (2017) BCC Evaluation and predictability analysis of seasonal prediction by BCC Second-Generation Climate System Model [C]//The 34th Annual Meeting of China Meteorological Society. S6 East Asian climate multi time scale variation mechanism and climate prediction. Zhengzhou: China Meteorological Society: 19.
37. Ren T , Li D C , Muller J , et al (2021) Sensitivity of radiative flux simulations to ice cloud parameterization over the equatorial western Pacific Ocean region [J]. *Journal of Atmospheric Sciences*. 78(8): 2549-2571. [doi:https://doi.org/10.1175/JAS-D-21-0017.1](https://doi.org/10.1175/JAS-D-21-0017.1)
38. Ren H L (2006) Strategies and methods for dynamic similarity forecasting [D]. Lanzhou: Lanzhou University.
39. Saha S (1992) Response of the NMC MRF model to systematic error correction eitin integration [J]. *Monthly Weather Review*. 120:345-360
40. Saha S, Moorthi S, Wu X, Wang J, et al (2014) The NCEP climate forecast system Vversion 2 [J]. *Journal of Climate*. 27: 2185–2208. <https://doi.org/10.1175/JCLI-D-12-00823.1>
41. Saha S, Nadiga S, Thiaw C, et al (2006) The NCEP Climate Forecast System. *Journal of Climate* [J]. 19:3483–3517. <https://doi.org/10.1175/JCLI3812.1>
42. Tao S Y, Chen L X (1987) A review of recent research of the East Asian summer monsoon in China [J] // Chang C P, Krishnamurti T N, Eds. *Monsoon Meteorology*. Oxford: Oxford University Press: 60–92.
43. Tao S Y, Wei J (2006) The westward, northward advance of the subtropical high over the west Pacific in summer [J]. *Journal of Applied Meteorological Science*. 17(5): 513–525. (in Chinese) <https://doi.org/CNKI:SUN:YYQX.0.2006-05-000>
44. Tao S Y, Zhu W M, Zhao W (1988) Interannual variability of Meiyu rainfalls [J]. *Chinese Journal of Atmospheric Sciences*, 12(s1): 13-21.
45. Vitart F, Ardilouze C, Bonet A, et al (2017) The Sub-seasonal to Seasonal Prediction (S2S) Project Database [J]. *Bull Amer Meteor Soc*. 98(1):163–173. <https://doi.org/10.1175/BAMS-D-16-0017.1>
46. Wang H J, He S P (2015) The North China/northeastern Asia severe summer drought in 2014[J]. *J. Climate*, 28 (17): 6667–6681. <https://doi.org/10.1175/JCLI-D-15-0202.1>.
47. Wang Z Y, Ding Y H (2008) Climatic characteristics of rainy seasons in China [J]. *Chinese Journal of Atmospheric Sciences*. 32(1):1–13. <https://doi.org/10.3878/j.issn.1006-9895.2008.01.01>



48. Wei F Y, Huang J Y (2010) A study of predictability for summer precipitation on east China using downscaling techniques [J]. *Journal of Tropical Meteorology*. 26(4):483-488.
49. Wei F Y, Song Q Y (2005) Spatial distribution of the global sea surface temperature with interdecadal scale and their potential influence on Meiyu in middle and lower reaches of Yangtze river [J]. *Acta Meteorologica Sinica*. 63(4):477-484.
50. Wei J, Zhang Q Y, Tao S Y (2003) Characteristics of atmospheric circulation anomalies during persistent droughts in North China for last two decades [J]. *Journal of Applied Meteorological Science*. 14(2):140-151.
51. Wu J, Ren H L, Zhang S, et al (2017) Evaluation and predictability analysis of seasonal prediction by BCC Second-Generation Climate System Model [J]. *Chinese Journal of Atmospheric Sciences*. 41(6): 1300-1315. [doi: 10.3878/j.issn.1006-9895.1703.16256](https://doi.org/10.3878/j.issn.1006-9895.1703.16256)
52. Wu Q, Zhan M J (2020) Climatic characteristics of hourly precipitation (1978–2019) in the Poyang Lake Basin, China [J]. *Geomatics Natural Hazards & Risk*. 11(1):1679-1696. <https://doi.org/10.1080/19475705.2020.1809535>
53. Wu Q, XU B, Wang Y H, et al (2021) Intraseasonal evolution and climatic characteristics of hourly precipitation during the rainy season in the Poyang Lake Basin [J]. *Geomatics Natural Hazards & Risk*. 12(1):1931-1947. <https://doi.org/10.1080/19475705.2021.1953619>
54. Wu T W, Qian Z A (2000) Further analyses of the linkage between winter and spring snow depth anomaly over Qinghai-Xizang Plateau and summer rainfall of Eastern China [J]. *Acta Meteorologica Sinica*. 58(5):570-581.
55. Xu H M, He J H, Zhou B (2001) The features of atmospheric circulation during Meiyu onset and possible mechanisms for westward extension (northward shift) of Pacific subtropical high [J]. *Journal of Applied Meteorological Science*. 12(2):150-158.
56. Xu Z, Fan K, Wang H (2015) Decadal variation of summer precipitation over China and associated atmospheric circulation after the late 1990s [J]. *Journal of Climate*. 28(10):4086-4106.
57. Yang J, Zhao J H, Zheng Z H, et al (2012) Estimating the prediction errors of dynamical climate model on the basis of prophase key factors in North China [J]. *Chinese Journal of Atmospheric Sciences*. 36(1):11-22.
58. Yang M Z, Ding Y H (2007) A study of the impact of South Indian Ocean Dipole on the summer rainfall in China [J]. *Chinese Journal of Atmospheric Sciences*, 31(4): 685-694.
59. Yu L L, Chen H S (2012) Possible Linkages among Anomalous Land Surface Condition, Surface Heating in Qinghai-Xizang Plateau in April and Summer Precipitation in China. *Plateau Meteorology* [J]. 31(5):1173-1182.
60. Yu X C, Zhao J H, Yang L et al (2019) The relationship between the onset date of the rainy season in North China and the atmospheric circulation and SST [J]. *Chinese Journal of Atmospheric Sciences*,43(1):107-118. <https://doi.org/10.3878/j.issn.1006-9895.1801.17242>.
61. Zhang F H, Chen T, Zhang F, et al (2020) Extreme features of severe precipitation in Meiyu period over the middle and lower reaches of Yangtze river basin in June-July 2020 [J]. *Meteorological Monthly*.

46(11):1405-1414.

62. Zhang Q Y, Tao S Y (1998) Influence of Asian mid high latitude circulation on East Asian summer rainfall [J]. *Acta Meteorologica Sinica*. 56(2):199–211. <https://doi.org/10.11676/gqxb1998.019>.
63. Zhang Q Y, Tao S Y (1998) Tropical and subtropical monsoon over east Asia and its influence on the rainfall over eastern China in summer [J]. *Quarterly Journal of Applied Meteorological Science*. 9(S1):17-23.
64. Zhang S L, Tao S Y (2001) The influences of snow cover over the Tibetan Plateau on Asian Summer Monsoon [J]. *Chinese Journal of Atmospheric Sciences*. 25(3): 372-390.
65. Zhao Z G (2000) Drought, flood and environmental field in summer of China [M]. Beijing: China Meteorological Press.
66. Zhao S Y, Chen L J, Cui T (2017) Effects of ENSO phase-switching on rainy-season precipitation in North China [J]. *Chinese Journal of Atmospheric Sciences*. 41(4): 857–868. <https://doi.org/10.3878/j.issn.1006-9895.1701.16226>.
67. Zhao S Y, Chen L J, Cui T (2017) Effects of ENSO phase-switching on rainy-season precipitation in North China[J]. *Chinese Journal of Atmospheric Sciences*. 41(4):857-868.
68. Zheng Z H, Ren H L, Huang J P (2009) Analogue correction of errors based on seasonal climatic predictable components and numerical experiments [J]. *Acta Physica Sinica*. 58(10):7359-7367.
69. Zhu J, Shukla J (2013) The role of air–sea coupling in seasonal prediction of Asia–Pacific summer monsoon rainfall [J]. *Journal of Climate*. 26:5689–5697. <https://doi.org/10.1175/JCLI-D-13-00190.1>

## Figures

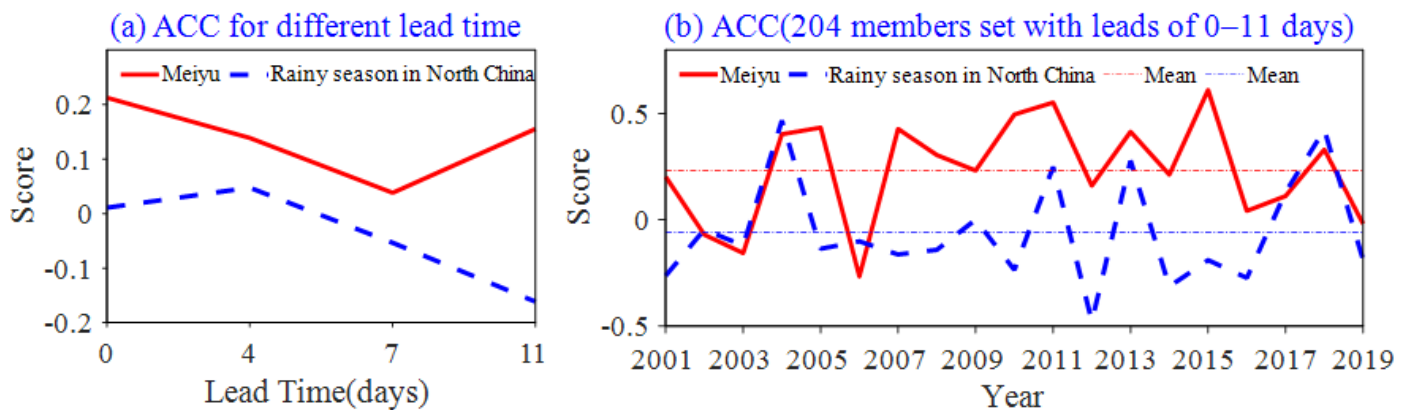
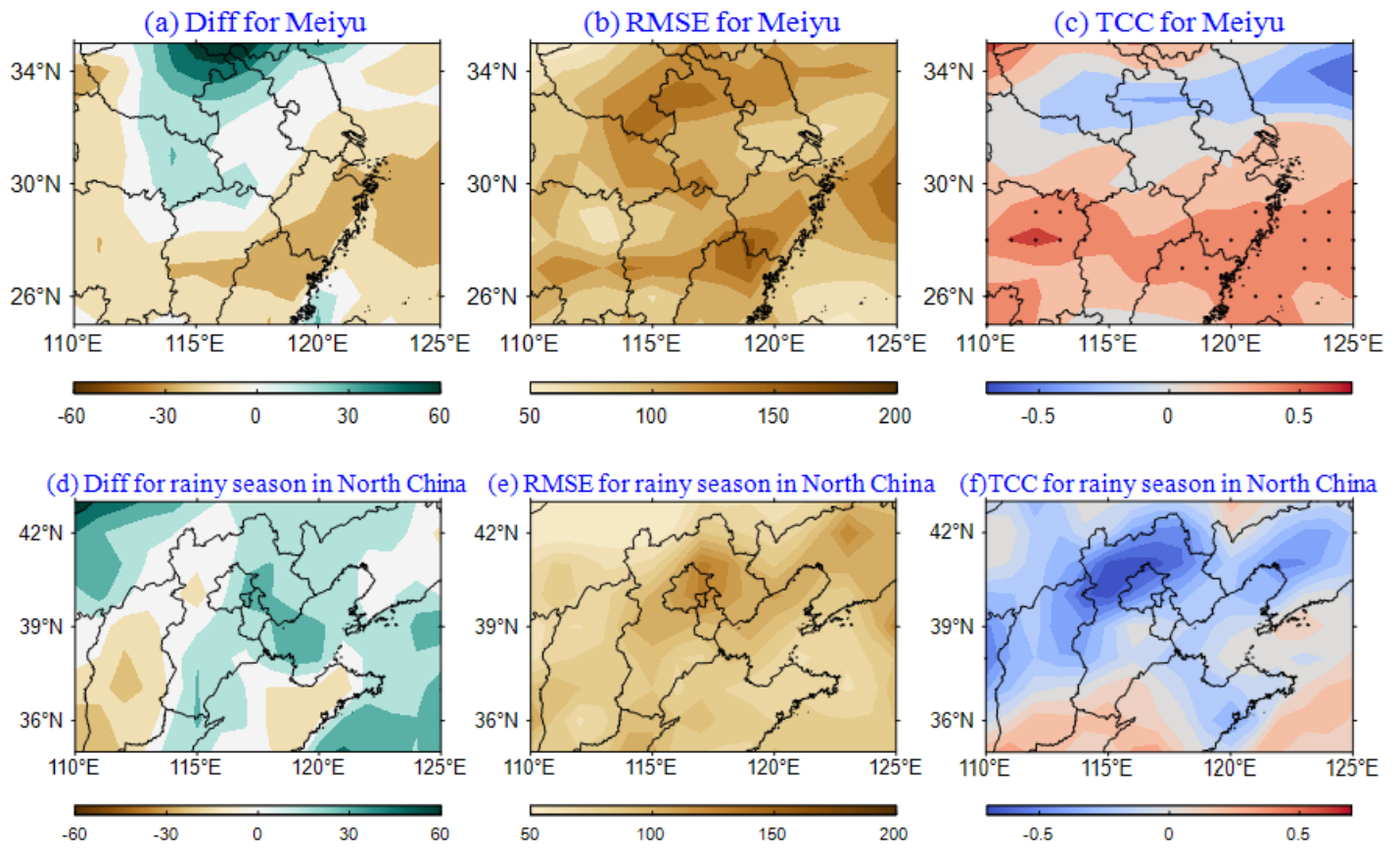


Figure 1

ACCs between ERA-Interim and S2S precipitation predictions for 2001–2019. (a) Annual average for different lead times; and (b) ensemble forecasts averaged annually.



**Figure 2**

DIFFs(%), RMSEs, and TCCs between ERA-Interim and S2S precipitation during (a-c) Meiyu and (d-f) rainy season in North China.

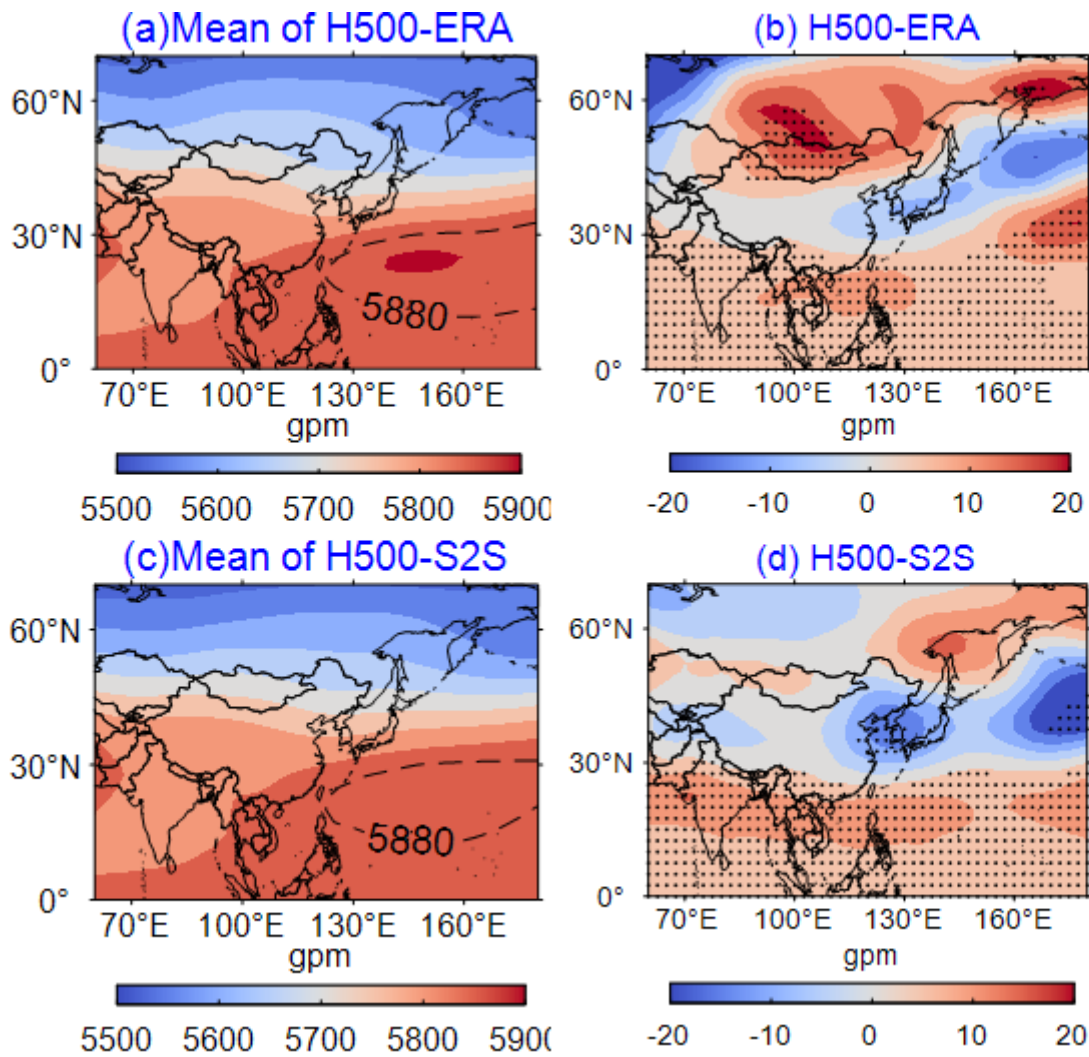


**Figure 3**

(a) 500-hPa height average field, and (b) regression of the 500-hPa height anomaly field onto the precipitation index during Meiyu in ERA-Interim. c and d are the same as a and b, but for S2S. The dots represent areas significant at 95% confidence level.

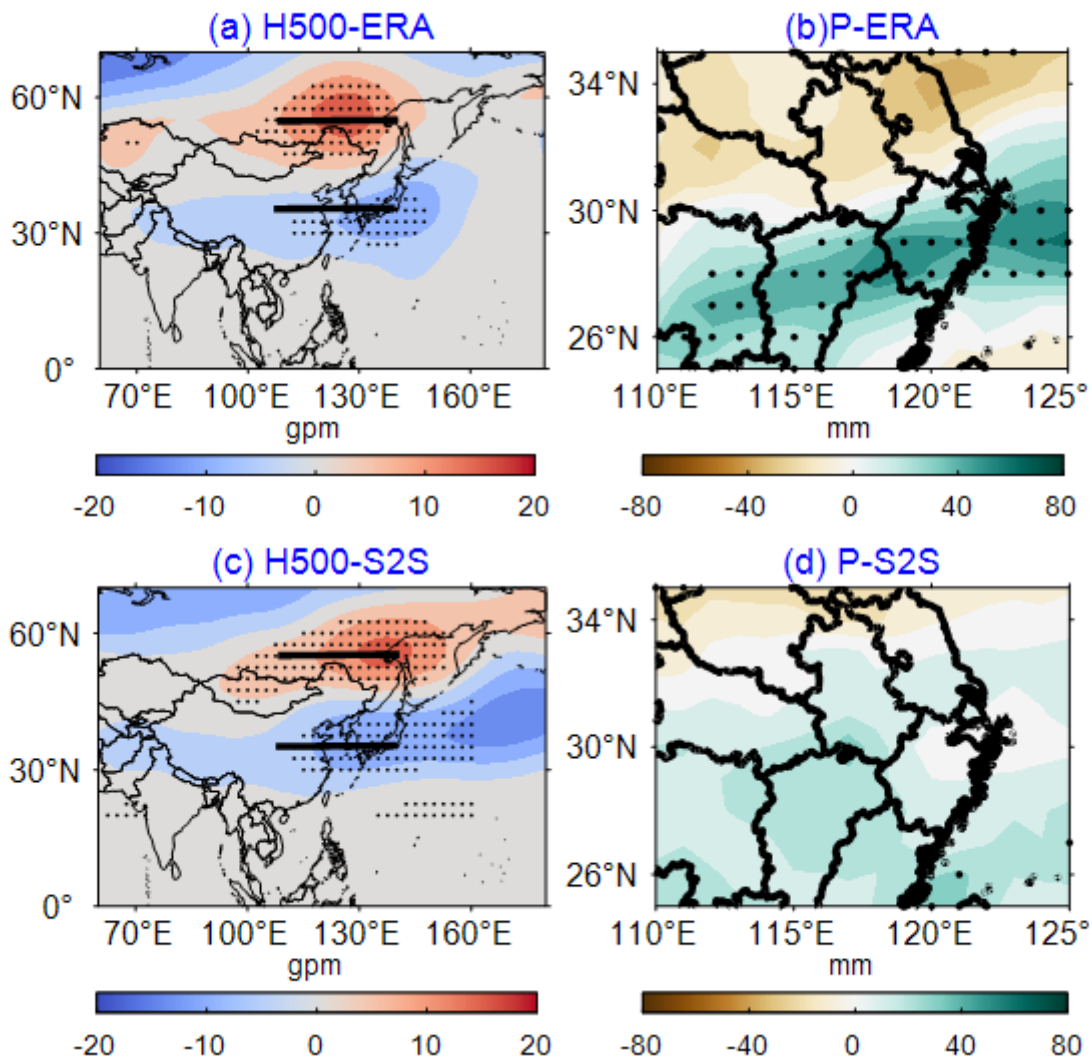


**Figure 4**

Regression of the 500-hPa height anomaly field (a) and the precipitation field (b) onto the index BHP during Meiyu in ERA-Interim. c and d are the same as a and b, but for the S2S. The dots represent areas significant at 95% confidence level.

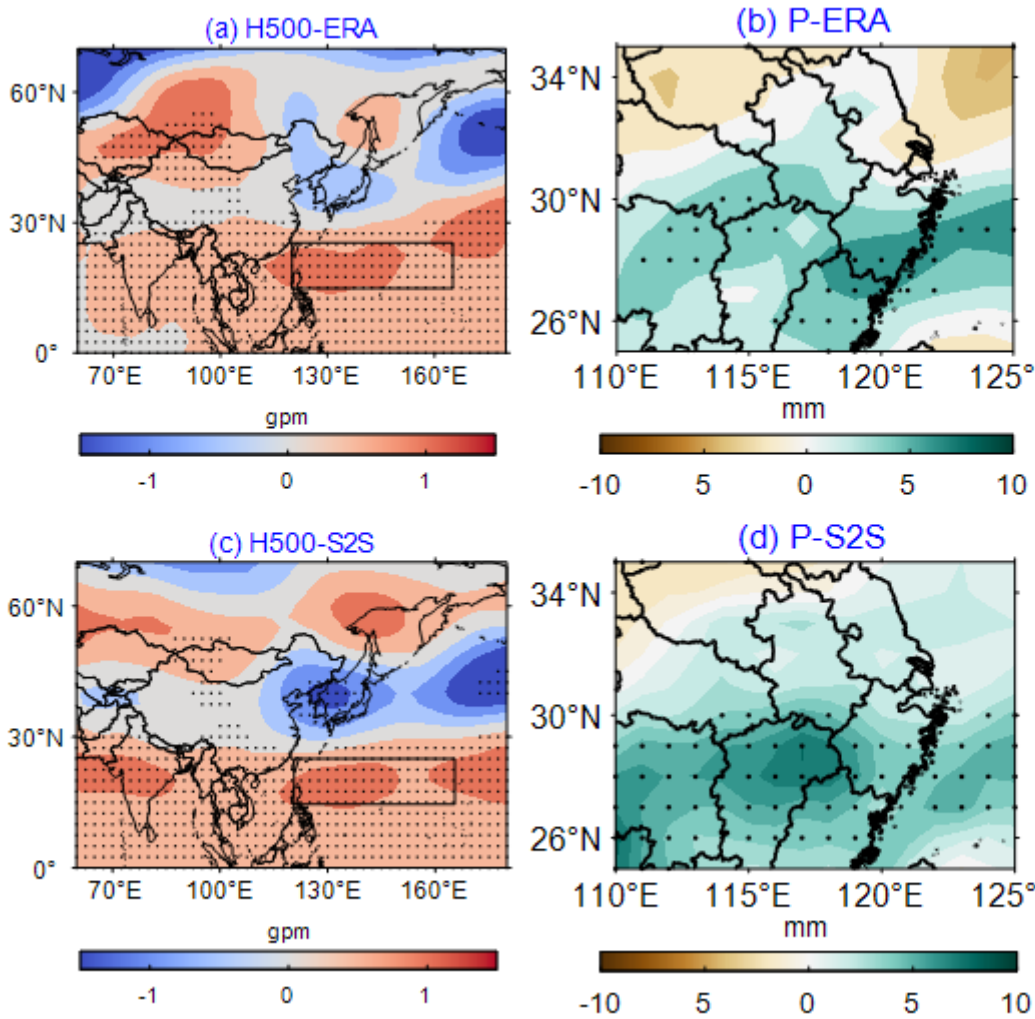


**Figure 5**

Regression of the 500-hPa height anomaly field (a) and precipitation field (b) onto the index SH during Meiyu in ERA-Interim. c and d are the same as a and b, but for the S2S. The dots represent areas significant at 95% confidence level.

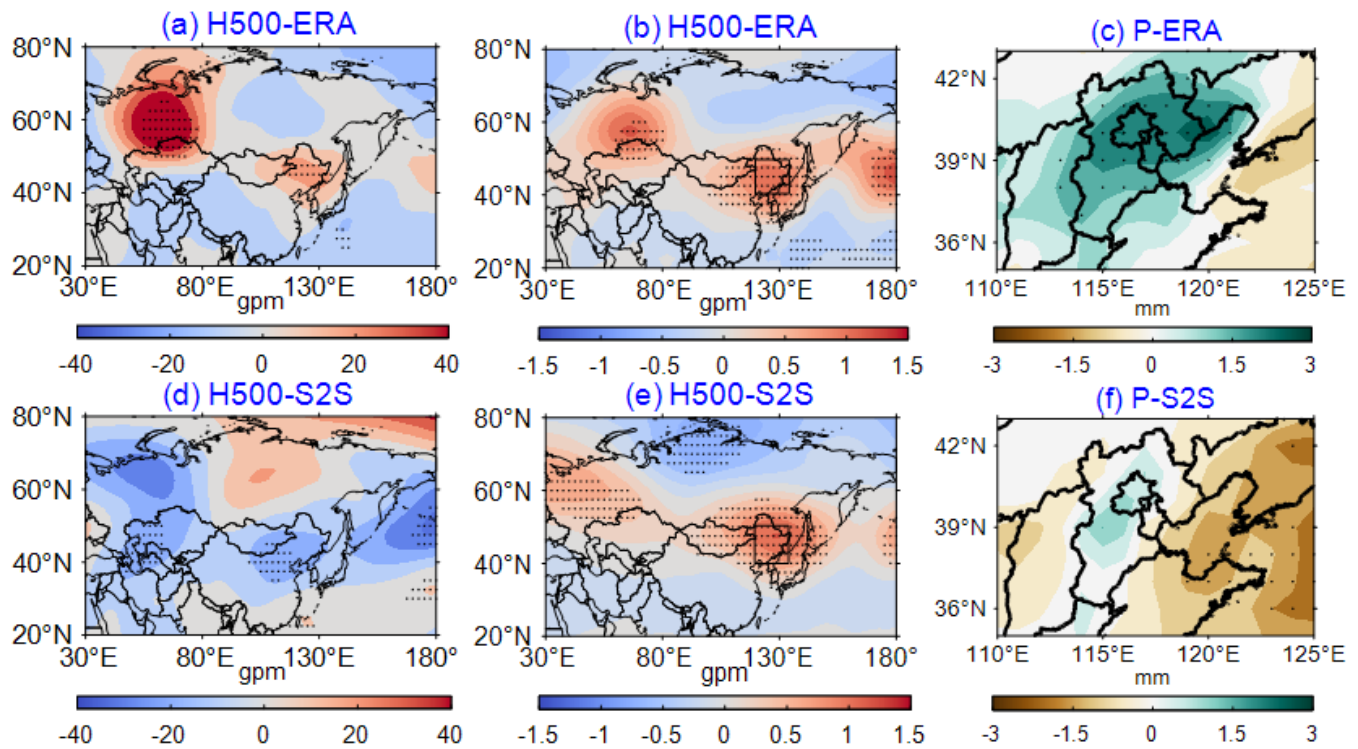


**Figure 6**

Regression of the 500-hPa height anomaly field (a) onto the precipitation index and the 500-hPa height anomaly field (b) and the precipitation field (c) onto the index HP during the rainy season in North China in ERA-Interim. d-f are the same as a-c, but for S2S.

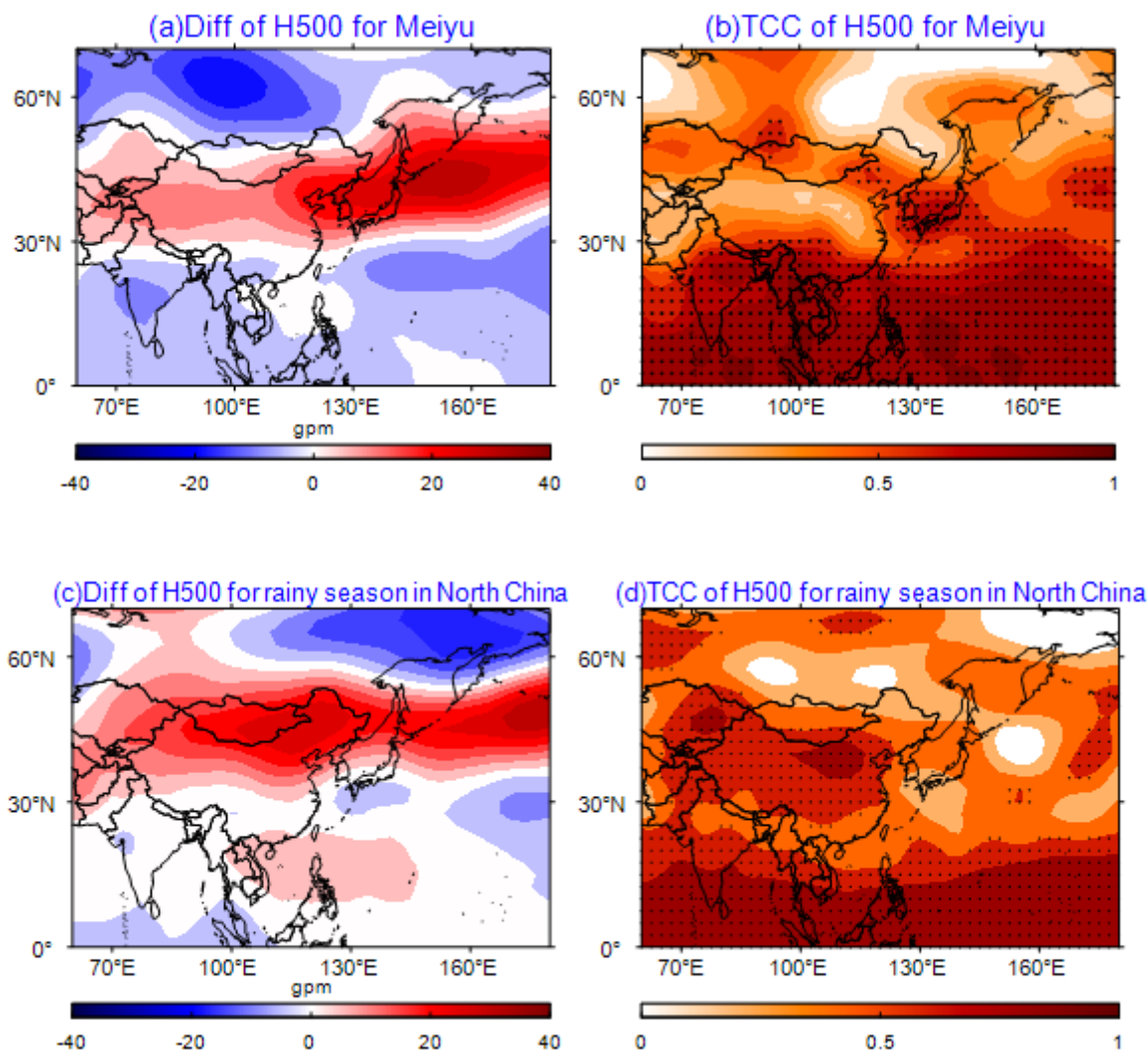


**Figure 7**

Deviation (a) and TCC (b) between the 500 hPa height from ERA-Interim and S2S predictions during Meiyu for 2001–2019. c-d are the same as a-b, but for the rainy season in North China.



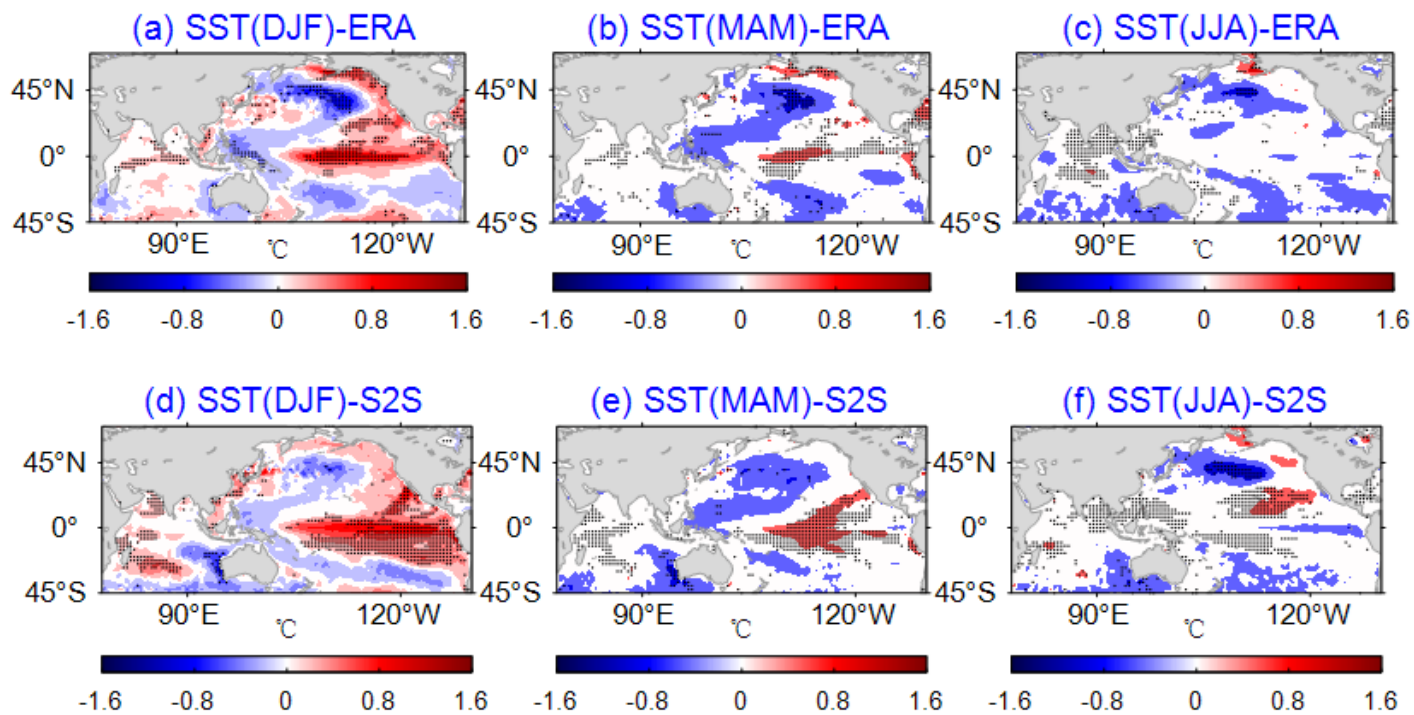


**Figure 8**

Regression of the sea surface temperature in the previous winter (a), spring (b) and summer (c) onto the precipitation index during Meiyu in the ERA-Interim. d-f are the same as a-c, but for the S2S. The dots represent areas significant at 95% confidence level.

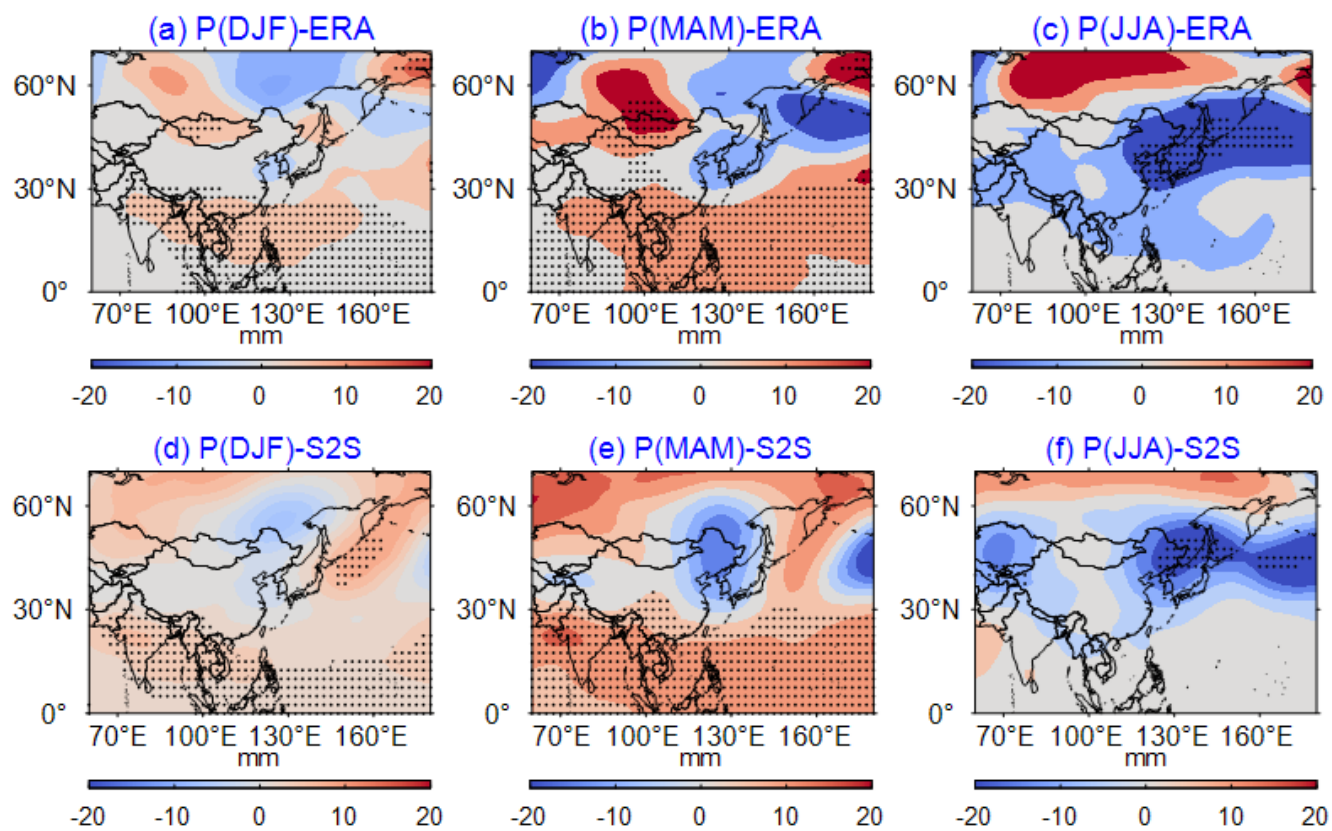


**Figure 9**

Regression of the 500-hPa height anomaly field onto the Niño3.4 index in the previous winter (a), spring (b) and summer (c) during Meiyu in the ERA-Interim. d-f are the same as a-c, but for the S2S. The dots represent areas significant at 95% confidence level.

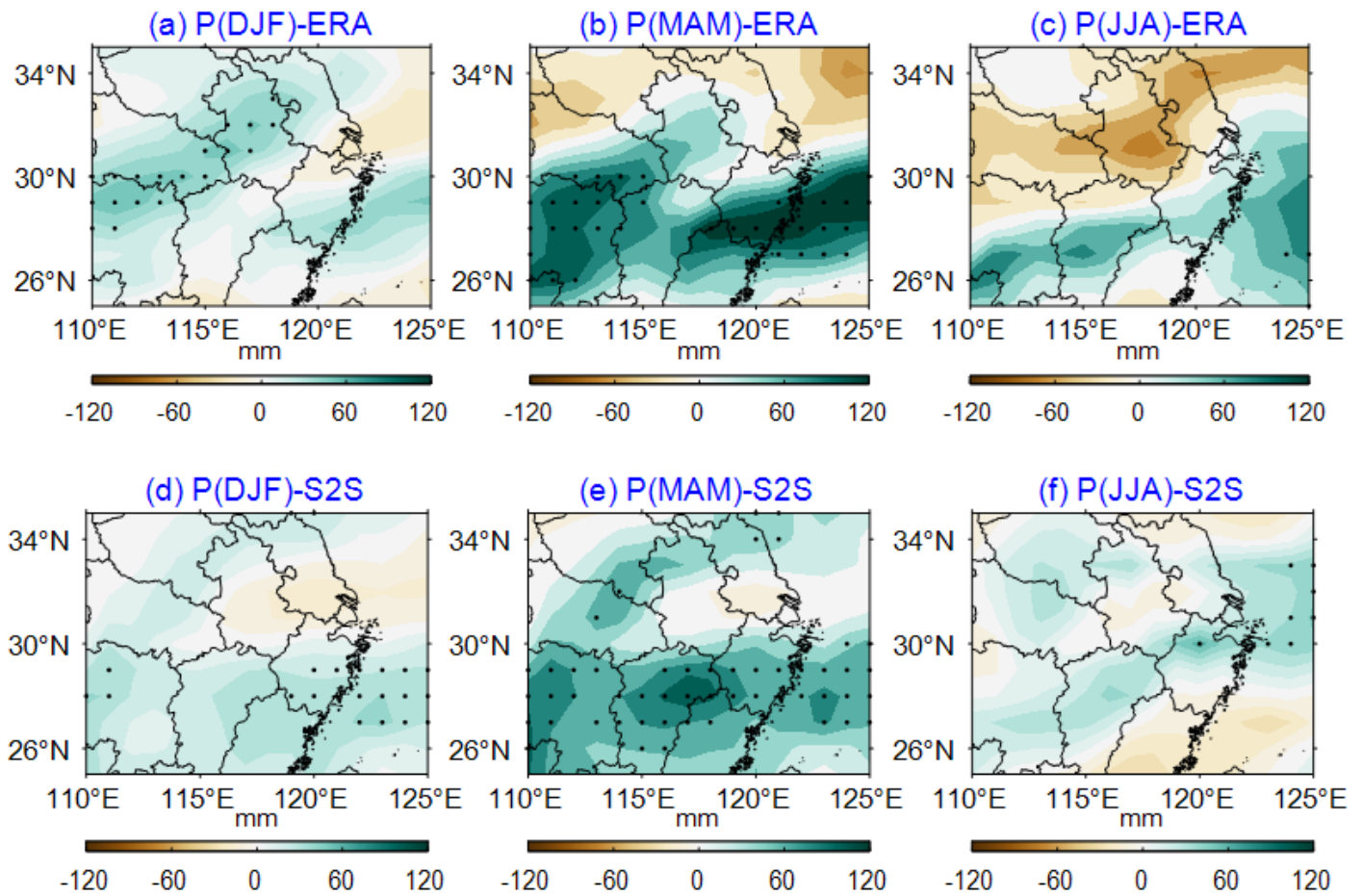


**Figure 10**

Regression of precipitation fields onto the Niño3.4 index in the previous winter (a), spring (b) and summer (c) during Meiyu in the ERA-Interim. d-f are the same as a-c, but for the S2S. The dots represent areas significant at 95% confidence level.

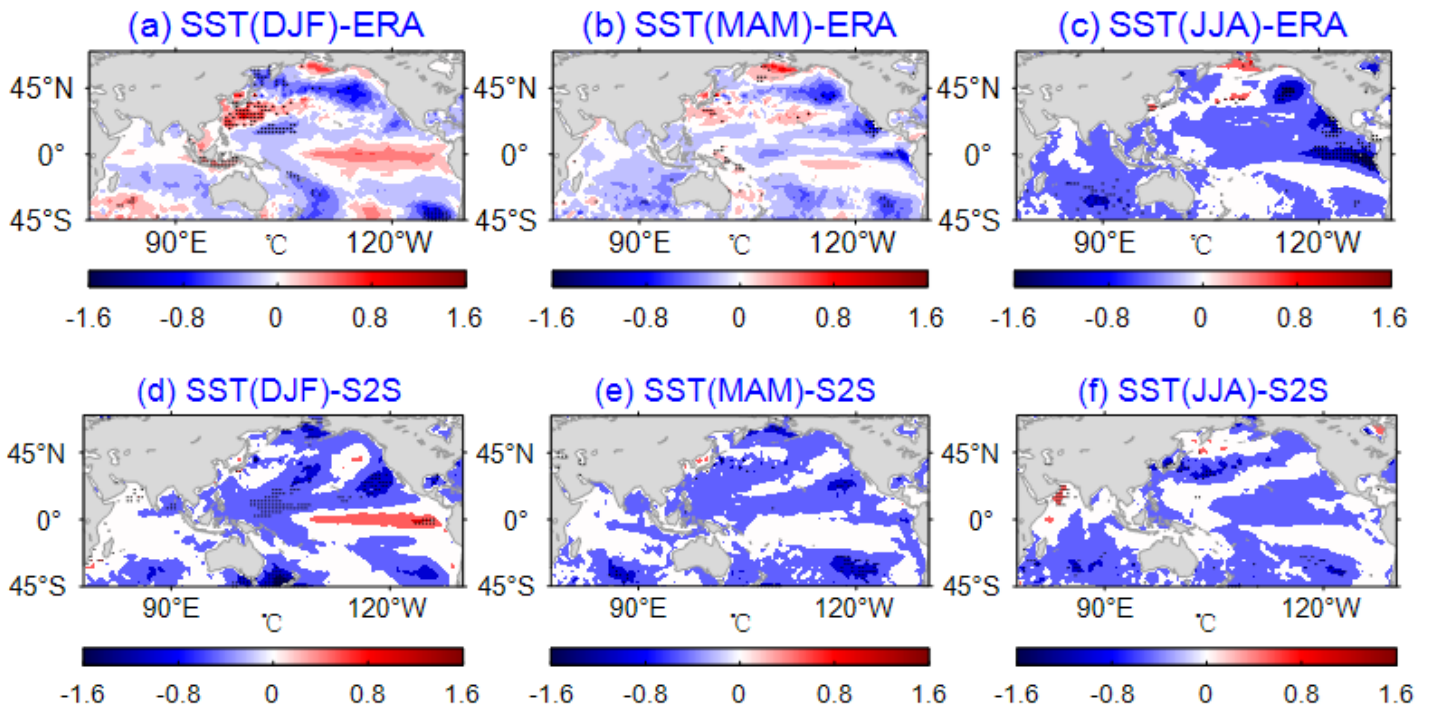


**Figure 11**

Regression of the SST in the previous winter (a), spring (b) and summer (c) onto the precipitation index during the rainy season in North China from ERA-Interim. d-f are the same as a-c, but for the S2S.